Freeze-dried dressing based on recombinant human-like collagen and EGF enhanced cutaneous wound healing in rats

Yangfan Li[1], Yating Cheng[1], Shiyi Huang[1], Fenglin Yu[1], Yu Bei[1], Yifan Zhang[1], Jianzhong Tang[1], Yadong Huang[1], and Qi Xiang[1]

[1]Jinan University

May 5, 2020

Abstract

Wound healing is a complex biological dynamic process that involves the transfer of multiple growth factors (GF) from the extracellular matrix (ECM) to fibroblasts for migration, proliferation, and wound closure. Among them, epidermal growth factor (EGF) as the most representative GF has been studied in deeply. Collagen is the most abundant ECM structural protein and has been widely used in tissue engineering for skin repair and skin remodeling. A recombinant human-like collagen (RHC) has been constructed to substitute nature collagen to improve its solubility and immunogenicity. We combined RHC and EGF to obtain a freeze-dried dressing to mimic the function of ECM for skin repair. A synergy occurred when combined EGF and RHC, that was significantly promoted the proliferation, adhesion and extension of fibroblasts (NIH/3T3) and migration of keratinocytes (HaCaT). RHC/EGF freeze-dried dressing was a loose and porous cake and redissolved quickly. RHC/EGF freeze-dried dressings significantly accelerated wound closure, re-epithelialization, orderly arrangement and deposition of collagen in the Sprague-Dawley rats with full-thickness skin defects. Further molecular mechanisms involved to cell proliferation and angiogenesis were carried out. The cell proliferation biomarkers (Ki67 and PCNA) and angiogenesis biomarkers (VEGF and CD31) were significantly up-regulated treated with RHC/EGF freeze-dried dressing. These findings demonstrated RHC/EGF freeze-dried dressing would be a potential therapeutic strategy in wound management.

1. Introduction

Assisting wounds healing with high efficacy is a research hotspot in the regenerative medicine. (Ying et al., 2019) In recent years, various types of wound-dressing materials containing growth factors to biomimetic extracellular matrix (ECM) have been more widely adopted to accelerate wound perfectly healing.(Choi et al., 2018; Thönes et al., 2019) Although extensive studies have been carried out around skin repair, but developing newer biodegradable dressings to promote wound healing are still enormous market demand.(Zoe, Elizabeth, June, & Louise, 2019) In particular, epidermal growth factor (EGF) plays key roles in skin wound repair.(J. et al.) Besides, as the most abundant ECM structural protein, collagen has good biocompatibility and degradability, and are considered as a better constituent for wound dressing preparations.(Davison-Kotler, Marshall, & Garcia-Gareta, 2019) We constructed a freeze-dried dressing based on recombinant human-like collagen (RHC) and EGF to confer a multifunctional product which can improve cell-biomaterial interactions and promote wound healing.

EGF is a typical growth factor that has been studied more in wound repair, which can bind to cell membrane receptors and exert various biological effects.(Duy et al.; Jones & Rappoport) In terms of the mechanism for promoting wound healing, one is that EGF are very powerful and can significantly promote keratinocytes and so on, and thus migrate to the injured site;(Jones & Rappoport; Schreier, Gekle, & Grossmann) the other is that as a mitogenic promoter, EGF promotes epithelial cell proliferation and division, improves collagen construction and regulates protein synthesis, thereby accelerating wound healing.(Berlanga-Acosta; Bodnar & J.; Lian & Li) In brief, EGF plays an essential role in wound healing .

Among recently available dressings, collagen-based dressings have shown to actively influence the healing process by intervening with various tissue components(Giriprasath et al.). Type I collagen can form fibrils through heterogeneous self-assembly compared with type II and type III collagen. (Irawan, Sung, Higuchi, & Ikoma, 2018; Jiang et al., 2016; Tiku & Madhan, 2016) Therefore, it is widely used as a biological material other than type II and type III collagen.(Sharma et al., 2017) However, the application of natural type I collagen is limited for its insolubility in water and poor processability. With the development of gene engineering, a series of highly hydrophilic, safe and effective recombinant human-like collagen (RHC) had attracted extensive attention worldwide. Many reports have been reported to expressed recombinant truncated type I human-like collagen peptides in*E.coli* ,(Guo et al., 2010; Yang et al.) whereas some of studies expressed recombinant type I human-like collagen peptides containing multiple identical motifs by means of codon optimization.(Olsen et al., 2005; Yao, Yanagisawa, & Asakura, 2004) Because these motifs are ligands for some types of integrin receptors, recombinant type I human-like collagen peptides is not only expected to enhance cell activity through certain integrin receptor binding, but also is extensible in various fibrous structural materials, including dressing.(Grab, Miles, Furcht, & Fields, 1996; Mashiko et al., 2018)

In this study, RHC consisting of cell adhesion domains derived from native type I collagen were designed and constructed by a genetic engineering method to construct a new type of RHC to overcome the deficiency of natural animal collagen. In addition, we prepared RHC/EGF freeze-dried dressing, and its potential applications for wound healing and repair were investigated using an*in vivo* full-thickness skin defects. Our results demonstrate that RHC/EGF freeze-dried dressing are a potentially useful tool for wound healing applications.

2. Materials and methods

2.1. Reagents

Escherichia coli BL21 (DE3) and plasmids containing pET-3c, an ampicillin-resistance gene, and isopropyl β-D-1-thiogalactopyranoside (IPTG) were provided by Invitrogen (Carlsbad, CA). Plasmid extraction and gel recovery kits as well as restriction enzymes and ligase were purchased from Guangzhou Tianjin Biotechnology Co., Ltd. (China). EGF were supplied by Jinan University Biopharmaceutical R&D Center (Guangzhou, China). All other reagents were provided by GBCBIO Technologies Inc. (Guangdong, China).

NIH/3T3 (ATCC CRL-7724) cells were purchased from Chinese Academy of Sciences (Shanghai, China) and cultured in RPMI 1640 supplemented with 10% fetal bovine serum (FBS) (Gibco, New York, USA). HaCaT cells (ATCC CRL-2310) were purchased from Chinese Academy of Sciences and cultured in DMEM supplemented with 10% FBS. All cell culture plates and bottles were obtained from Corning Company (Corning, NY).

2.2. Construction and identification of recombinant human-like collagen

The gene encoding RHC was cloned into the pET-3c expression vector to generate a recombinant plasmid named pET3c-hlcollagen, which was transformed into *E. coliBL21(DE3*). After screening for ampicillin resistance and induction by IPTG, the best expression condition was selected. Lager scale production of RHC was performed using a 50L fermenter. And RHC protein was purified using affinity chromatography on a NI Sepharose 6 Fast Flow column combined with gel filtration Sephadex G-25. PCR, western blot, and gel electrophoresis were used for identification of RHC.

2.3. Cell proliferation assays

Proliferation of EGF, RHC and RHC/EGF were assessed using an MTT assay. NIH/3T3 cells (3×10^3 cells/well) were seeded into 96-well plates. After 24 h of culture, the medium was changed to maintenance medium (MEM with 0.4% FBS), and the cells underwent starvation for 6 h. The cells were then cultured in maintenance medium containing 0, 0.5, 1, 2, 4, 8 or 16 nmol/L RHC, EGF or RHC/EGF for 48 h. The effect of RHC, EGF or RHC/EGF on NIH/3T3 cells proliferation was detected by the MTT assay according to the manufacturer's instructions. Briefly, 20 μL of 0.5% MTT solution was added to each well in the dark, and the cells were incubated at 37°C in a 5% CO_2atmosphere for 4 h. After removal of the medium, 100

μL of dimethyl sulfoxide was added, and the absorbances at 570 nm were measured in a microplate reader (MK3, Thermo, Waltham, MA, USA). Each assay was performed in triplicate.

2.4. Cell Migration Assay

An *in vitro* scratch wound healing model was used to assess cell migration. HaCaT cells were plated in a 12-well plate and grown to complete fusion. Next, they were scraped in a straight line with a 100-μL pipette tip to create a uniform cell-free zone and rinsed three times with PBS. Then the cells were treated with normal medium or medium containing EGF or RHC/EGF. The images of the cells at the beginning and at regular intervals during cell migration to close the scratch were captured and compared through quantifying the migration rate of the cells.

2.5. Cell adhesion assays

Cell adhesion activity was measured using the crystal violet assay. 96 well plates were coated with 1noml/mL of EGF, RHC and RHC/EGF overnight at 4. After washing with phosphate-buffered saline (PBS), the wells were blocked with 1% (w/v) bovine serum albumin for 30 min. NIH/3T3 cells were seeded in the same plates at 6 $\times 10^3$ cells per well in FBS-free medium. After 2h, cells were washed twice with PBS and fixed with Methanol solution for 20 min at room temperature. Fixed cells were stained with 1% (w/v) crystal violet (Solarbio, China) for 30min at 37. Stained cells were then gently washed three times with PBS. Cell images were captured by MF53 microscope (Mshot, Guangzhou, China). The experiment was performed in quintuplicate, and the number of adherent cells was calculated from the images captured at five positions per well to determine the average. For cell lysis, 1% SDS solution was added. The absorbance was measured using a microplate reader at 570nm.

2.6. Cytoskeleton staining assays

12-well plate cell were coated with 1noml/mL of EGF, RHC and RHC/EGF at 4 overnight. After washing with phosphate-buffered saline (PBS), the wells were blocked with 1% (w/v) bovine serum albumin for 30 min. NIH/3T3 cells were seeded in the same plates at 4 x10^4 cells per well in FBS-free medium. After 4h, cells were washed with PBS and fixed for 10 min with 4% paraformaldehyde solution, and then washed with PBS. Cells were stained with a phalloidin (1:200, Solarbio, China) for 30 min at 37 in the dark. The cells were washed three times with PBS to remove unbound phalloidin. Cells were stained with DAPI (1:1000, Beyotime, China) for 5 min at room temperature. The samples were washed three times with PBS to remove unbound DAPI. Images were collected using the LSM 700 confocal LASER scanning microscope (ZEISS, German), with excitation wave lengths of 488 and 561 nm. Analyze the image with image J to calculate the cell adhesion area

2.7. Preparation and characterization of RHC and RHC/EGFfreeze-dried dressing

2.7.1 Preparation of RHC and RHC/EGF freeze-dried dressing

RHC, EGF and RHC/EGF (1: 1) were lyophilized separately to obtain freeze-dried dressing. In short, the configured RHC and RHC/EGF solutions were subjected to gradient cooling, respectively. Place at 4degC for 1 hour, then at -20 for 6 hours, and finally at -80 overnight. Next, the frozen RHC, EGF and RHC/EGF were vacuum freeze-dried at -50. The freeze-dried dressing was sterilized by Co60 and stored in a sterile dry sealed EP tube for further experiment purpose.

2.7.2 Characterization of RHC and RHC/EGF freeze-dried dressing

The morphologies and properties of the freeze-dried dressing were characterized by scanning electronic microscope (SEM). Before the SEM observation, the freeze-dried dressing was subjected to gold sputtering using a gold spray carbonator, and the micromorphology of RHC and RHC/EGF freeze-dried dressing was observed by scanning electron microscopy (SEM, XL30; Philips, Amsterdam, The Netherlands).

2.7.3 RHC and RHC/EGF freeze-dried dressing rehydration time

RHC and RHC/EGF freeze-dried dressing solubility tests were performed by using physiological saline. In short, we dissolved RHC and RHC/EGF freeze-dried dressing with 300μl of physiological saline. Determine whether the liquid can be sufficiently dissolved by the degree of liquid clarification, and record the dissolution time. All these physical measurements were made in triplicate at 25.

2.8. In vivo studies in full-thickness skin defect SD rat model

All SD rats (60d postnatal) used in this study were purchased from the animal center of Guangdong province (No. 44007200069979) and caged under controlled room temperature, humidity, and light (12/12-h light-dark cycle) with access to water and food ad libitum. The experimental protocols used in this study were approved by the Institutional Animal Care and Use Committee of Jinan University (Approval number: 2019228). All experiments were conducted according to the guidelines for animal care and use of China, and they were approved by the animal ethics committee of the Chinese Academy of Medical Science. Establish a full-thickness skin defect model and evaluate role of the RHC, EGF, RHC/EGF freeze-dried dressing in the wound healing. Female SD rats (200 ± 20g, n = 80) were randomly assigned to four groups: (1) Control group (treated with physiological saline), (2) EGF group, (3) RHC group, (4) RHC/EGF group. In short, rats were anesthetized with an intraperitoneal injection of 10% chloral hydrate, and their backs were shaved and cleaned with ethanol. A whole-skin defect model was prepared with a 1.8-cm diameter ring drill to compress a circular mark (2.54 cm^2), and then the skin was cut off along the mark. Wounds were treated with physiological saline, EGF, RHC or RHC/EGF freeze-dried dressing.

2.9 Macroscopic evaluation of wounded tissues

For measurement of wound closure percentage, wounds were photographed at 0, 3, 7, 10, 14, and 21 d post-wounding and analyzed by using ImageJ software. The wound area was measured by the limits of grossly evident epithelialization. The wound closure percentage at each time point was derived by the following formula: [(Initial wound size-current wound size)/initial wound size×100].

2.10. Microscopic evaluation of H&E-stained samples

On days 3, 7, 14, and 21 after surgery, the rats were sacrificed, and the wound samples together with a surrounding rim of normal skin were harvested. For histological analysis, the samples were first fixed in 4% neutral buffered paraformaldehyde, sequentially dehydrated in a series of ethanol with increasing gradient concentration, and cleared by the exposure to xylene. Then, the samples were incubated with paraffin xylene solution in an oven overnight, to remove the xylene, and embedded in paraffin. The paraffin-embedded samples were sectioned at the thickness of 8.0 μm to adhere to glass slides. After the process of dewaxing and hydration, the sections were stained with H&E for routine examination. Then, Masson's trichrome staining was performed to further analyze the characteristics of these wound samples. Sections were analyzed, and images were captured by microscopy (Olympus IX71, Tokyo, Japan). H&E stained samples were used to measure the thick ratio of epithelial thickness at 14 and 21 d post-wounding.

2.11 Immunohistochemical analysis of wound cell proliferation

At 3 and 14 d, wound tissue specimens harvested from wound-healing model rats were used for immunohistochemical evaluation. Immunohistochemical staining of vascular endothelial growth factor (VEGF) and CD31 were performed using a streptavidin-biotin method. In brief, sections were dewaxed and microwaved for 10 min to retrieve antigens, and then endogenous peroxidase was blocked by incubation in 3% hydrogen peroxide for 30 min in the dark. Sections were permeabilized with 1% Triton solution and blocked in 5% bovine serum albumin. Next, sections were incubated with antibodies against VEGF (1:300 dilution, GB14165, Google Biotechnology) and CD31 (1:200 dilution, GB11063-3, Google Biotechnology) overnight. After rinsing with PBS, sections were incubated with rabbit secondary antibody for 40 min. After washing four times with PBS, DAB and hematoxylin were applied for coloration and re-dying of the nucleus, respectively. Finally, sections were dehydrated and sealed with Permount™ Mounting Medium for microscopic observation (Olympus IX71, Tokyo, Japan).

2.12. Wound Angiogenesis by Immunofluorescence

At 7 and 21 d, wound tissue specimens harvested from wound-healing model rats were used for immunohistochemical fluorescence evaluation. To visualize immunofluorescence, sections were incubated with antibodies against Ki67 (1:300 dilution, GB13030-2, Google Biotechnology) and proliferating cell nuclear antigen (PCNA, 1:200 dilution, GB11010, Google Biotechnology) overnight. After rinsing with PBS, sections were incubated with a fluorescent rabbit secondary antibody for 40 min. After washing four times with PBS, cell nuclei were stained by DAPI, and images were acquired with a confocal laser-scanning microscope (Olympus, LSM 700, Japan).

2.13. Statistical analysis

All data were expressed as mean ± standard deviation (SD) of at least three independent experiments. Statistical analyses were performed using GraphPad Prism 6 software (GraphPad Software Inc., La Jolla, CA, USA). Differences among more than two groups were analyzed by one-way ANOVA followed by a Tukey HSD comparison test. Values of $P < 0.05$ were considered statistically significant.

3. Results and Discussion

3.1. Construction and identification of recombinant human-like collagen

Using genetic engineering technology, we constructed RHC according to the construction schematic shown for recombinant plasmid of pET3c-hlcollagen in Fig. 1A. The results from nucleic acid electrophoresis in Fig. 1B showed that the RHC gene was successfully ligated into the expression vector. After induction of *E.coli*BL21 containing recombinant plasmid RHC with IPTG at either 30 °C or 37 °C for 4h, or 20 °C overnight, soluble RHC was expressed at the highest level at 37 °C (Fig. 1C). Subsequently, RHC protein was purified using affinity chromatography on a NI Sepharose 6 Fast Flow column combined with gel filtration Sephadex G-25. Purity of RHC were detected by SDS-PAGE gel electrophoresis (Fig. 1D) and western blot (Fig. 1E), and in both of them a single band was obtained. Identity were confirmed by MALDI-TOF MS and HPLC-based peptide mapping (the data were not shown). We conducted at least three consecutive batches of 50L fermentation process tests, and the mean of RHC protein expression accounted for 48% of the total protein in the bacterial cell supernatant (the data were not shown).

3.2.RHC/EGF promotes proliferation and migration

Fibroblast proliferation is critical for rapid closure of wounds during wound healing. We performed cell proliferation experiments on NIH/3T3 cells to detect the proliferative activity of RHC, EGF and RHC/EGF. Cell proliferation experiments found that RHC did not promote the proliferation of NIH/3T3 cells. But EGF and RHC/EGF (1: 1) can significantly promote cell proliferation (Fig. 2A). On the other hand, Keratinocytes (HaCaT cell) are essential for effective re-epithelialization and ECM construct during wound healing(Piperigkou, G?tte, Theocharis, & Karamanos). HaCaT cell are regarded as a good *in vitro* model of the skin epidermal layer, and can be used to assess the therapeutic effects of compounds on tissue regeneration.(Burlando et al.) *In vitro* wound healing assay using a created wound gap by HaCaT cells showed that, in RHC and RHC/EGF group, wound closures by cell migration in HaCaT cell were significantly promoted compared to those of non-treatments or EGF group (Fig. 2B). After 12 h and 24 h incubation in HaCaT cells, markedly higher wound closure percentages were monitored. The migration characteristics of HaCaT cells on RHC, EGF, and RHC/EGF were examined by scratch wound assay (Fig. 2B). After 24 h incubation in HaCaT cells, a significantly higher wound closure percentages were monitored in RHC (78 ± 3.12%) and RHC/EGF (91.6 ± 1.62%) versus those in Control (46.3 ± 1.82%) and EGF (62.3 ± 2.12%), showing a significant difference (P ¡0.01) (Fig. 2C). The proliferation and migration of fibroblasts and keratinocytes play a vital role in the rapid healing of wounds. Experiments show that RHC has no obvious effect on the proliferation of NIH/3T3 cells, but can significantly promote HaCaT cell migration. In contrast, EGF can significantly promote NIH/3T3 cells, but has no obvious effect on HaCaT cell migration. When we combined RHC and EGF, we found that they have a synergistic effect. RHC/EGF can both promote the proliferation of NIH/3T3 cells and migrate HaCaT cells. Among them, RHC/EGF and EGF have similar activities to promote the proliferation of NIH/3T3 cells. Surprisingly, compared with RHC and EGF, RHC/EGF has a significant effect on promoting HaCaT cell migration. This is beneficial for accelerating wound healing.

These data also clearly show that RHC/EGF have the potential for use in cell therapies to treat cutaneous wounds.

3.3. RHC- EGF promote NIH/3T3celladhesion and extension

It has long been known that cell adhesion importantly influences the cell proliferation, migration, differentiation, and even the assembly of individual cells into the three-dimensional tissues of animals.(Gumbiner, 1996) To investigate the effect of RHC, EGF or RHC/EGF on cell adhesion, NIH/3T3 cells were cultured in serum free medium and plated on 96-well plates coated with RHC, EGF or RHC/EGF for 2 h. The cell adhesive activity of the NIH/3T3 cells was then evaluated by crystal violet assay. As shown in Fig. 2D, RHC and RHC/EGF groups found to significantly promoted cell adhesion compared with the control and EGF groups. Among them, the RHC/EGF group had the largest number of cells attach and were well-spread and exhibited the typical fibroblast cell morphology. We also determined the average number of cells that attached to monolayers presenting control, RHC, EGF and RHC/EGF (Fig. 2E). The largest number of cells attached to RHC/EGF, with approximately 130 cells attached per field of view. This significant decrease in adhesion at control and EGF reveals, attachment dropped to 20-30 cells per field.

To further analyze the adhesion activity of RHC/EGF to NIH/3T3 cells. In a separate experiment, we allowed cells to adhere for four hours to each of the monolayer substrates and then fixed and stained the samples to compare the development of the cytoskeleton (Fig. 2F). We observed that cells spread well on the RHC/EGF surfaces, and these cells also displayed organized actin cytoskeletons spanning the entire cells, indicating that the biological adhesion between them and substrates experienced a progression from substrate attachment, spreading, and cytoskeleton development. In contrast, we found a lack of organized actin structures in cells attached to control and EGF. In order to quantify the spread of attached cells, we calculated the cell area by image J (Fig. 2G). The results show that the spread area of NIH/3T3 cells in RHC/EGF is significantly larger than that of control and EGF. These results indicated that RHC/EGF has considerable adherent activity on NIH/3T3 cells. Previous studies revealed that collagen, the major structural protein found in the ECM of many tissues, is rich in arginine-glycine-aspartic acid (RGD), a cell adhesion motif that is capable of promoting cell adhesion.(Shekhter, Fayzullin, Vukolova, Rudenko, & Litvitsky, 2019) RHC we construct through genetic engineering has RGD. We speculate that exposure to RGD is the main factor that accounts for the enhancement of cell adhesion by RHC.

3.4 Characterization of RHC/EGF freeze-dried dressing

Scanning electron microscopy results of RHC and RHC/EGF (1: 1) freeze-dried dressing are shown in Fig. 3. RHC and RHC/EGF freeze-dried dressing had an obvious but irregular pore structure, which facilitated substance exchange between cells and freeze-dried dressing. However, compared with RHC freeze-dried dressing, RHC/EGF freeze-dried dressing self-assemble by lyophilization to form a distinct fiber structure. This is very similar to the natural ECM structure. Conducive to the rapid integration of wound skin during wound repair, and accelerate the speed and effect of skin wound repair. In addition, solubility experiments show that RHC and RHC/EGF freeze-dried dressing have good solubility. Both can be completely dissolved in physiological saline in a short time (3~5 s), forming a transparent and uniform aqueous solution and easy-to-use.

3.5. Wound-Healing effect of RHC/EGF forfull-thickness skin defects in Vivo

We separately lyophilized EGF, RHC and RHC/EGF to obtain freeze-dried dressing. After establishing the full-thickness skin defects model, the wounds were treated with RHC and RHC/EGF freeze-dried dressing respectively. Wounds treated with EGF served as a positive control group, while physiological saline was administered to the control group. Wound closure results at each time point in each experimental group are shown in Fig. 4A. Healing time of the RHC/EGF group was obviously reduced compared with that of the other groups, and the wound closure rate of the RHC/EGF group was much higher than that of the other two groups. These results indicated that RHC/EGF increased the healing capability of wounds compared with RHC or EGF. At 10 days post-wounding, a significantly higher wound closure percentage was monitored in EGF (88.39 +- 4.13%) and RHC/EGF (90.33 +- 7.47%) versus closure in RHC (69.32 +-

6.18%) and control (65.79 +- 9.48%), showing a significant difference (P ¡0.01) (Fig. 4B). The appearances of the wounds indicated that RHC/EGF freeze-dried dressing was an optimal wound dressing for accelerating early healing of skin wounds. Importantly, RHC/EGF freeze-dried dressing improved wound appearance, whereas non-treatment developed noticeable large and elongate scars.

Then, the histological analysis was further investigated via H&E staining to assess the quality of the newly formed skin tissue (Fig. 4C). Early in the process of wound healing, the reduction of inflammatory cells and the presence of more capillaries in the damaged skin are beneficial to speeding up wound repair. At 3d, H&E staining results indicated relief of wound inflammation and significant capillary growth in the RHC/EGF group, while there were large amounts of inflammatory cells infiltrating into the upper layer of dermis in the control and there were almost no capillaries. Re-epithelialization is an important stage of wound repair. Through re-epithelialization, the wound area is continuously reduced until the wound is completely closed and a new dermal layer is completely formed.(Xiao, Reis, Feric, Knee, & Radisic, 2016) Evaluation of the skin-injury model after treatment for 14 and 21 d (Fig. 4D) indicated significantly increased epithelial thickness in the RHC/EGF group (41.66 +- 4.62μM,P ¡0.01) compared with control (26.83 ± 3.58μM) and RHC groups(32.33 ± 3.18μM).

3.6. Skin collagen regeneration and orderly arrangement

Collagen is the main component of the extracellular matrix and provides tensile strength to the skin.(Rowley, Nagalla, Wang, & Liu) It regulates cell proliferation and migration during wound healing and plays an important role in wound contraction.(Xinhua et al., 2019) Masson's trichrome staining can be used to observe the deposition and morphology of collagen to assess the overall quality of the scar area. Masson's trichrome staining results showed that the wound treated with RHC exhibited deposition of ECMs on 7d, especially for collagen stained as blue (Fig. 4E). In addition, at 21 d, more collagen deposition on the surface of wounds treated with RHC/EGF and collagen fibers within the wound areas of the RHC/EGF were more compact and arranged, as compared to those in the control group. These results revealed that RHC/EGF can not only relieve wound inflammation and elicit significant capillary growth but can also improve epithelial thickness and collagen fiber expression, which are beneficial to wound healing without scars.

3.7. RHC/EGF accelerates cell proliferation in wound skin

In full-thickness skin defect model, the cell proliferation activity in the wound can directly reflect the rate of wound healing and regenerative capacity. Ki67 and PCNA, as nuclear antigens related to proliferating cells, are important biomarker proteins for measuring cell proliferative activity. By detecting changes in its expression level, it can directly reflect the proliferation level of cells in the damaged skin. At 3 and 14 d, damaged skin tissues were collected to detect expression of two cell proliferation-specific proteins, Ki67(Brown & Gatter, 2002) and PCNA(Boehm, Gildenberg, & Washington, 2016), as shown in Fig. 5. After treatment for 3 d, expression of Ki67 and PCNA were significantly upregulated in the RHC/EGF group (Fig. 5A and C). Statistical results show that there is a significant difference between the RHC/EGF group and the Control group. This shows that RHC/EGF can accelerate wound healing by promoting cell proliferation in wound skin (Fig. 5 B and D); As the wounds healed, their expression was downregulated in all groups at 14 d.

3.8. RHC/EGF promotes neovascularization of wound skin

Neovascularization is necessarily required for normal tissue development, particularly to provide oxygen and nutrition to granulation tissues. CD31 is found on the surface of endothelial cells and is widely used as a marker of angiogenesis.(Camila et al.) VEGF, as a marker of angiogenesis, can enhance vascular permeability and promote the formation of capillaries in new blood vessels.(Jelena et al.) Damaged skin was collected on days 3 and 14 and the expression of CD31 and VEGF in vascular network was assessed by IHC (Fig. 6). After treatment for 3 or 14 d, expression of CD31 was significantly increased in EGF and RHC/EGF groups compared with control and RHC groups. At the same time points, VEGF expression exhibited the same trend. As angiogenesis biomarkers, upregulation of CD31 and VEGF demonstrates that RHC/EGF can accelerate wound healing and repair. Therefore, RHC/EGF freeze-dried can promote wound healing

by promoting angiogenesis. Local application of growth factors such as bFGF, EGF, and VEGF are the most common methods to promote wound healing by promoting angiogenesis.(Qu et al.; Xue, Zhao, Lin, & Jackson) However, skin defect repair is a complex process that requires the synergistic effects of cell adhesion, spread, migration, and angiogenesis. As a result, many of these growth factors fail to achieve complete wound healing. In addition, collagen has a good role in promoting cell adhesion and migration, but has the disadvantages of poor solubility and easy to cause immune response Therefore, we prepared RHC/EGF freeze-dried while promoting adhesion, diffusion, migration, and angiogenesis. In summary, RHC/EGF promotes cell adhesion, proliferation, migration, and angiogenesis in vitro. In vivo, RHC/EGF freeze-dried accelerate wound healing by enhancing re-epithelialization, promoting collagen deposition and angiogenesis. Therefore, RHC/EGF freeze-dried may be a promising dressing for wound healing.

4. Conclusion

In this study, RHC we constructed has a better effect on promoting cell adhesion. Simultaneously, we have successfully achieved the desire to produce RHC on a large scale. Compared with NIH/3T3 cells cultured on RHC or EGF alone, cells on RHC/EGF exhibited better adhesion, viability, and migration characteristics. This result indicated that the combination of both EGF and RHC has a synergistic effect. Observed by scanning electron microscopy, the RHC/EGF dressings we obtained by freeze-drying are more like natural collagen fibrous structure than the RHC dressing alone. Consequently, we investigated its potential application in wound healing and repair. In full-thickness skin defect SD rats model *in vivo* , we found that application of an RHC /EGF freeze-dried dressing could accelerate wound healing and repair compared with RHC, EGF or the control wound treatment. This repair manifested as upregulated expression of angiogenesis biomarkers VEGF and CD31 as well as cell proliferation-specific proteins Ki67 and PCNA. Collectively, these results support the therapeutic value of RHC freeze-dried dressing as a topical biomaterial dressing and EGF biocarrier for regenerative therapies. Thus, RHC/EGF freeze-dried dressing is a potentially useful tool for wound healing applications.

Acknowledgements

This work was supported by grants from Guangzhou Science and Technology Program Key Project [Grant No. 201803010044]; Science and Technology Program of Tianhe District, Guangzhou City [Grant No. 201704YG066]; and the Major Scientific and Technological Special Project of the Administration of Ocean and Fisheries of Guangdong Province [Yuecainong, 2017, No. 17; Grant No. GDME-2018C013].

Author Contribution statement

Qi Xiang and Yadong Huang designed the study. Yating Cheng and Yangfan Li performed experimental work. Yangfan Li, Fengli Yu and ShiYi Huang performed the data analyses. Yu Bei and Jianzhong Tang contributed materials. Yu Bei, ShiYi Huang, Yifan Zhang helped perform the analysis with constructive discussions. Yating Cheng and Yangfan Li wrote the manuscript. Qi Xiang and Yadong Huang modified the manuscript. Yating Cheng and Yangfan Li contributed equally to this work.

Declaration of interest

The authors report no conflicts of interest. The authors alone are responsible for the content and writing of this article.

References

Berlanga-Acosta, J. Diabetic lower extremity wounds: the rationale for growth factors-based infiltration treatment. *International wound journal, 8* (6), 612-620.

Bodnar, & J., R. Epidermal Growth Factor and Epidermal Growth Factor Receptor: The Yin and Yang in the Treatment of Cutaneous Wounds and Cancer. *Advances in wound care, 2* (1), 24-29.

Boehm, E. M., Gildenberg, M. S., & Washington, M. T. (2016). The many roles of PCNA in eukaryotic DNA replication. *Enzymes, 39* .

Brown, D. C., & Gatter, K. C. (2002). Ki67 protein: The immaculate deception? *Histopathology, 40* (1), 2-11.

Burlando, B., Ranzato, E., Volante, A., Appendino, G., Pollastro, F., & Verotta, L. Antiproliferative Effects on Tumour Cells and Promotion of Keratinocyte Wound Healing by Different Lichen Compounds. *Planta Medica, 75* (06), 607-613.

Camila, Couto, Figueiredo, Núbia, Braga, Pereira, . . . Ant?nio. Double immunofluorescence labeling for CD31 and CD105 as a marker for polyether polyurethane-induced angiogenesis in mice.

Choi, S. M., Lee, K. M., Kim, H. J., Park, I. K., Kang, H. J., Shin, H. C., . . . Lee, J. W. (2018). Effects of structurally stabilized EGF and bFGF on wound healing in type I and type II diabetic mice. *Acta Biomater, 66* , 325-334. doi:10.1016/j.actbio.2017.11.045

Davison-Kotler, E., Marshall, W. S., & Garcia-Gareta, E. (2019). Sources of Collagen for Biomaterials in Skin Wound Healing. *Bioengineering (Basel), 6* (3). doi:10.3390/bioengineering6030056

Duy, Dao, Lorenzo, Anez-Bustillos, Rosalyn, Adam, . . . Puder. Heparin-Binding Epidermal Growth Factor-Like Growth Factor as a Critical Mediator of Tissue Repair and Regeneration.

Giriprasath, Ramanathan, Sitalakshmi, Thyagarajan, Uma, Tiruchirapalli, & Sivagnanam. Accelerated wound healing and its promoting effects of biomimetic collagen matrices with siderophore loaded gelatin microspheres in tissue engineering.

Grab, B., Miles, A. J., Furcht, L. T., & Fields, G. B. (1996). Promotion of fibroblast adhesion by triple-helical peptide models of type I collagen-derived sequences.*J Biol Chem, 271* (21), 12234-12240. doi:10.1074/jbc.271.21.12234

Gumbiner, B. M. (1996). Cell Adhesion: The Molecular Basis of Tissue Architecture and Morphogenesis.*Cell, 84* (3), 345-357.

Guo, J., Luo, Y., Fan, D., Yang, B., Gao, P., Ma, X., & Zhu, C. (2010). Medium optimization based on the metabolic-flux spectrum of recombinant Escherichia coli for high expression of human-like collagen II. *Biotechnol Appl Biochem, 57* (2), 55-62. doi:10.1042/BA20100081

Irawan, V., Sung, T. C., Higuchi, A., & Ikoma, T. (2018). Collagen Scaffolds in Cartilage Tissue Engineering and Relevant Approaches for Future Development. *Tissue Eng Regen Med, 15* (6), 673-697. doi:10.1007/s13770-018-0135-9

J., Hardwicke, and, D., Schmaljohann, and, . . . D. Epidermal growth factor therapy and wound healing — past, present and future perspectives.

Jelena, Rakocevic, Dejan, Orlic, Olivera, Mitrovic-Ajtic, . . . Dobric. Endothelial cell markers from clinician's perspective.

Jiang, Y., Wang, H., Deng, M., Wang, Z., Zhang, J., Wang, H., & Zhang, H. (2016). Effect of ultrasonication on the fibril-formation and gel properties of collagen from grass carp skin. *Materials Science and Engineering: C, 59* , 1038-1046. doi:10.1016/j.msec.2015.11.007

Jones, S., & Rappoport, J. Z. Interdependent epidermal growth factor receptor signalling and trafficking. *International Journal of Biochemistry & Cell Biology, 51* , 23-28.

Lian, N., & Li, T. Growth factor pathways in hypertrophic scars: Molecular pathogenesis and therapeutic implications. *Biomedicine & Pharmacotherapy, 84* , 42-50.

Mashiko, T., Takada, H., Wu, S. H., Kanayama, K., Feng, J., Tashiro, K., . . . Yoshimura, K. (2018). Therapeutic effects of a recombinant human collagen peptide bioscaffold with human adipose-derived stem cells on impaired wound healing after radiotherapy. *J Tissue Eng Regen Med, 12* (5), 1186-1194. doi:10.1002/term.2647

Olsen, D., Jiang, J., Chang, R., Duffy, R., Sakaguchi, M., Leigh, S., . . . Polarek, J. W. (2005). Expression and characterization of a low molecular weight recombinant human gelatin: development of a substitute for animal-derived gelatin with superior features. *Protein Expr Purif, 40* (2), 346-357. doi:10.1016/j.pep.2004.11.016

Piperigkou, Z., G?tte, M., Theocharis, A. D., & Karamanos, N. K. Insights into the key roles of epigenetics in matrix macromolecules-associated wound healing.*Advanced drug delivery reviews* , S0169409X17302326.

Qu, Y., Cao, C., Wu, Q., Huang, A., Song, Y., Li, H., . . . Man, Y. The Dual-delivery of KGF and bFGF by Collagen Membrane to Promote Skin Wound Healing. *Journal of Tissue Engineering & Regenerative Medicine* .

Rowley, A. T., Nagalla, R. R., Wang, S.-W., & Liu, W. F. Extracellular Matrix-Based Strategies for Immunomodulatory Biomaterials Engineering. *Advanced healthcare materials* .

Schreier, B., Gekle, M., & Grossmann, C. Role of epidermal growth factor receptor in vascular structure and function. *Current Opinion in Nephrology & Hypertension, 23* (2), 113-121.

Sharma, U., Carrique, L., Vadon-Le Goff, S., Mariano, N., Georges, R.-N., Delolme, F., . . . Hulmes, D. J. S. (2017). Structural basis of homo- and heterotrimerization of collagen I. *Nature Communications, 8* (1). doi:10.1038/ncomms14671

Shekhter, A. B., Fayzullin, A. L., Vukolova, M. N., Rudenko, T. G., & Litvitsky, P. F. (2019). Medical Applications of Collagen and Collagen-Based Materials. *Current Medicinal Chemistry, 26* (3), 506-516.

Thönes, S., Rother, S., Wippold, T., Blaszkiewicz, J., Balamurugan, K., Moeller, S., . . . Saalbach, A. (2019). Hyaluronan/collagen hydrogels containing sulfated hyaluronan improve wound healing by sustained release of Heparin-Binding EGF-like growth factor. *Acta biomaterialia* .

Tiku, M. L., & Madhan, B. (2016). Preserving the longevity of long-lived type II collagen and its implication for cartilage therapeutics. *Ageing Res Rev, 28* , 62-71. doi:10.1016/j.arr.2016.04.011

Xiao, Y., Reis, L. A., Feric, N., Knee, E. J., & Radisic, M. (2016). Diabetic wound regeneration using peptide-modified hydrogels to target re-epithelialization. *Proc Natl Acad Sci U S A, 113* (40), E5792.

Xinhua, Liu, Chi, Zheng, Xiaomin, Luo, . . . Huie. (2019). Recent advances of collagen-based biomaterials: Multi-hierarchical structure, modification and biomedical applications.

Xue, M., Zhao, R., Lin, H., & Jackson, C. Delivery systems of current biologicals for the treatment of chronic cutaneous wounds and severe burns. *Advanced drug delivery reviews* , S0169409X18300413.

Yang, C., Hillas, P. J., B??ez, J. A., Nokelainen, M., Balan, J., Tang, J., . . . Polarek, J. W. The Application of Recombinant Human Collagen in Tissue Engineering.*Biodrugs Clinical Immunotherapeutics Biopharmaceuticals & Gene Therapy, 18* (2), 103-119.

Yao, J., Yanagisawa, S., & Asakura, T. (2004). Design, expression and characterization of collagen-like proteins based on the cell adhesive and crosslinking sequences derived from native collagens. *J Biochem, 136* (5), 643-649. doi:10.1093/jb/mvh172

Ying, H., Zhou, J., Wang, M., Su, D., Ma, Q., Lv, G., & Chen, J. (2019). In situ formed collagen-hyaluronic acid hydrogel as biomimetic dressing for promoting spontaneous wound healing. *Mater Sci Eng C Mater Biol Appl, 101* , 487-498. doi:10.1016/j.msec.2019.03.093

Zoe, M. R., Elizabeth, W. Z., June, C. A., & Louise, F. B. (2019). Development and use of biomaterials as wound healing therapies. *Burns & Trauma* (1), 1.

Figures:

Figures 1. Construction and identification of RHC. (A) Construction schematic of recombinant pET3c-hlcollagen plasmid. (B) Nucleic acid electrophoresis of recombinant plasmid pET3C-HLC. M: DNA Ladder

2000; lane 1: monoclone of recombinant plasmid pET3C-HLC; lane 2: negative control. (C) Effect of temperature on RHC expression, as analyzed by SDS-PAGE. RHC was induced by IPTG for 4 h at either 37 or 30 or overnight at 20. M: middle molecular weight protein markers; lanes 2, 4, and 6: RHC after induction at 20, 30, or 37; lanes 1, 3, and 5: RHC before induction. (D) SDS-PAGE analysis of proteins during purification. M: middle molecular weight protein markers; lane 1: broken by PBS; lane 2: Ni-NTA spin columns; lane 3: washed protein through 80 mM imidazole. (E) Western blotting analysis. M: middle molecular weight protein markers; lane 1: RHC with anti-His antibody.

Figures 2. Cell biological activity of RHC/EGF (1:1). (A) MTT assay of NIH/3T3 cell proliferation rates on RHC, EGF, or RHC/EGF. (B) Images obtained at 0, 12, and 24 h after wound creation in vitro migration assay on RHC, EGF, or RHC/EGF. (C) Quantitative analysis of gap area of HaCaT cells cultured on RHC, EGF, or RHC/EGF. (D) Optical micrographs of crystal violet stained NIH/3T3 cells adhering to monolayers presenting. (E) Quantitative detection of the number of NIH/3T3 cells adhering. (F) Cytoskeleton staining. (G) Quantitative calculation of cell spread area. n = 3, means +- SD, *P<0.05, **P<0.01 vs control group, ns means no significant difference vs. control, P >0.05.

Figures 3. Characteristics of RHC and RHC/EGF. (A) Scanning electron micrographs of RHC and RHC/EGF freeze-dried dressing.

Figures 4. Experimental study of rat wound-healing model after treatment with physiological saline, RHC, EGF, or RHC/EGF. (A) Wounds were photographed at 0, 3, 5, 7, 10, 14, and 21 d. (B) H&E staining of rat wound-healing model after treatment for 3, 14, and 21 d. (C) Quantitative analysis of epithelial thickness at 14 and 21 d using ImageJ software. (D) Quantitative analysis of wound closure rate. (E) Masson's trichrome staining of rat wound-healing model after treatment for 7 and 21 d. n = 6, means +- SD, *P<0.05, **P<0.01 vs control group, ns means no significant difference vs. control, P >0.05.

Figures 5. Immunofluorescence examination of Ki67 and PCNA expression. (A) Immunofluorescence examination of Ki67-positive cells after treatment for 7 and 21 d. Arrows indicate Ki67 expression. (B) Quantitative analysis of Ki67-expressing cells at 7 and 14 d measured using ImageJ software. (C) Immunofluorescence examination of PCNA-positive cells after treatment for 7 and 21 d. Arrows indicate PCNA expression. (B) Quantitative analysis of PCNA-expressing cells at 7 and 14 d measured using ImageJ software. n = 3, means +- SD, *P < 0.05, **P < 0.01, ***P < 0.001 vs control group, ns means no significant difference vs. control, P >0.05.

Figures 6. Immunohistochemical examination of CD31 and VEGF expression. (A) Immunohistochemical labeling of CD31-positive cells after treatment for 3 and 14 d. Arrows indicate CD31 expression. (B) Quantitative analysis of CD31-expressing cells at 3 and 14 d measured using ImageJ software. (C) Immunohistochemical labeling of VEGF-positive cells after treatment for 3 and 14 d. Arrows indicate VEGF expression. (D) Quantitative analysis of VEGF-expressing cells measured at 3 and 14 d using ImageJ software. n = 3, means SD, *P < 0.05, **P < 0.01, ***P < 0.001, ****P < 0.0001 vs control group, ns means no significant difference vs. control, P >0.05.

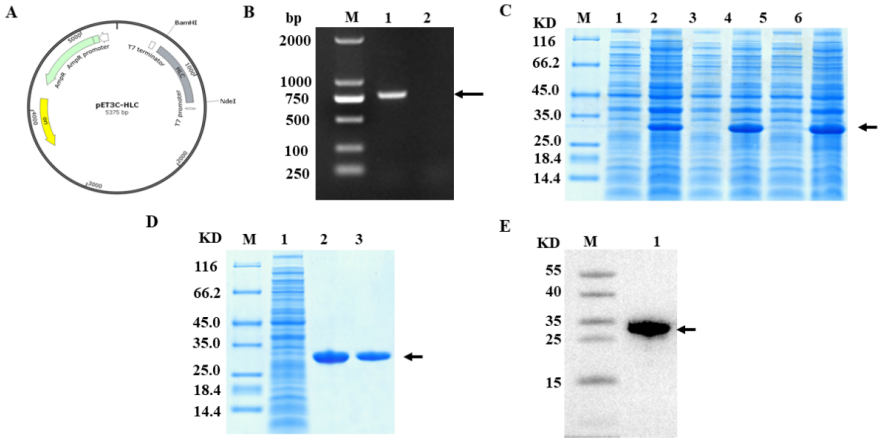

Figure 1

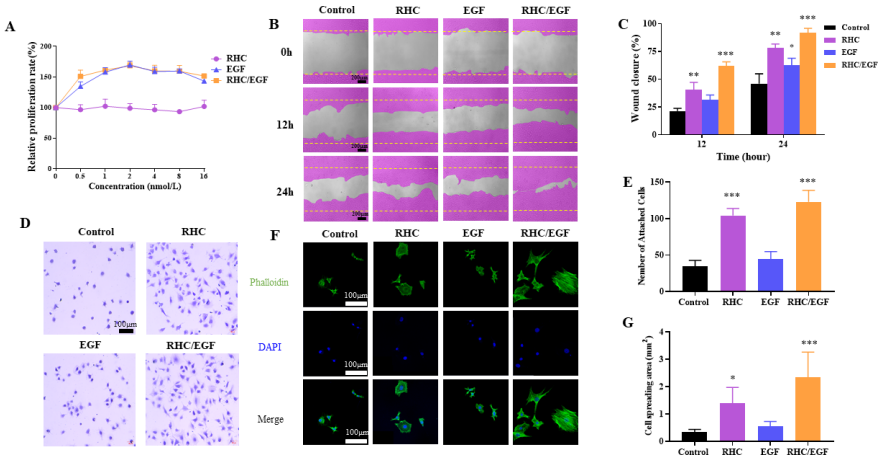

Figure 2

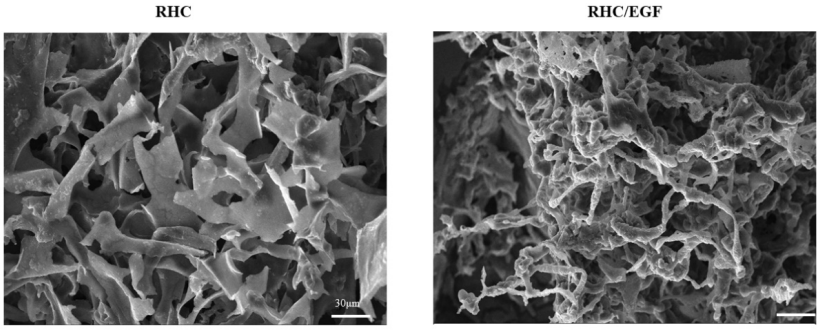

Figure 3

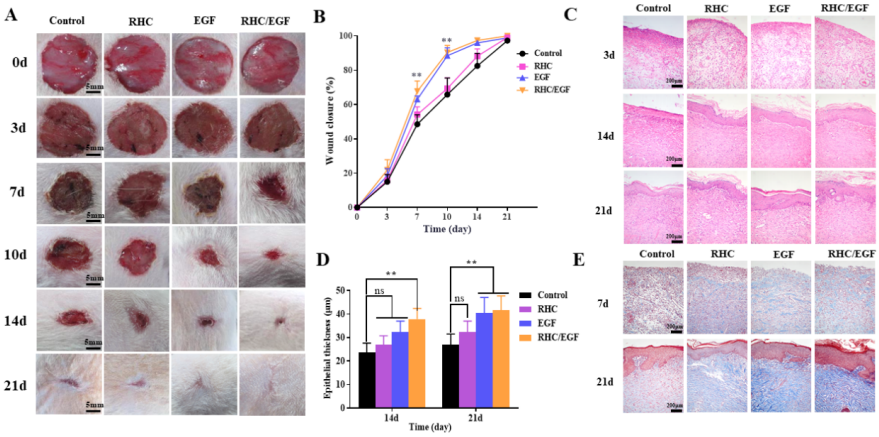

Figure 4

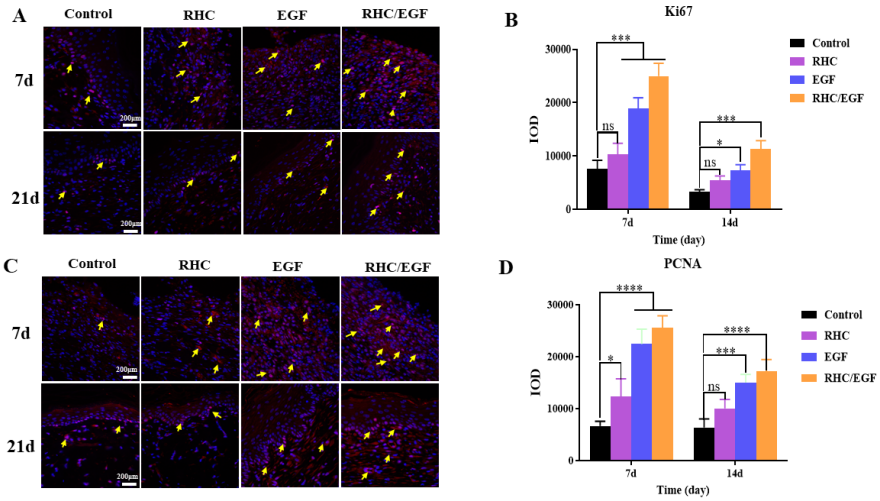

Figure 5

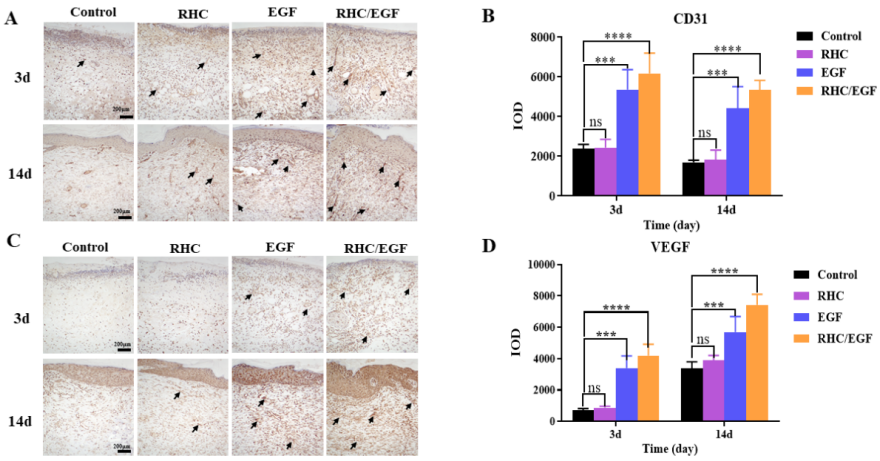

Figure 6

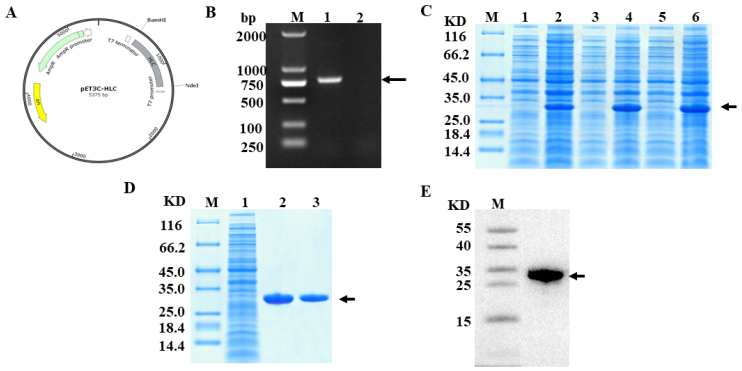

Fig. 1. Construction and identification of RHC. (A) Construction schematic of recombinant pET3c-hlcollagen plasmid. (B) Nucleic acid electrophoresis of recombinant plasmid pET3C-HLC. M: DNA Ladder 2000; lane 1: monoclone of recombinant plasmid pET3C-HLC; lane 2: negative control. (C) Effect of temperature on RHC expression, as analyzed by SDS-PAGE. RHC was induced by IPTG for 4 h at either 37°C or 30°C or overnight at 20°C. M: middle molecular weight protein markers; lanes 2, 4, and 6: RHC after induction at 20°C, 30°C, or 37°C; lanes 1, 3, and 5: RHC before induction. (D) SDS-PAGE analysis of proteins during purification. M: middle molecular weight protein markers; lane 1: broken by PBS; lane 2: Ni-NTA spin columns; lane 3: washed protein through 80 mM imidazole. (E) Western blotting analysis. M: middle molecular weight protein markers; lane 1: RHC with anti-His antibody.

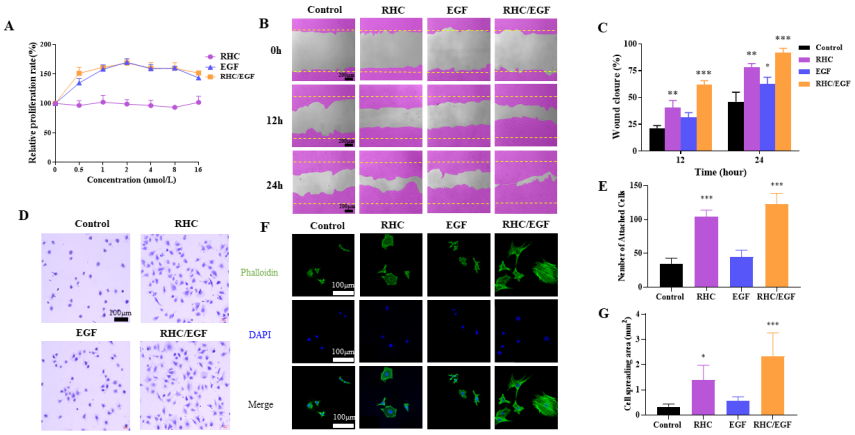

Fig. 2. Cell biological activity of RHC/EGF (1:1). (A) MTT assay of NIH/3T3 cell proliferation rates on RHC, EGF, or RHC/EGF. (B) Images obtained at 0, 12, and 24 h after wound creation in vitro migration assay on RHC, EGF, or RHC/EGF. (C) Quantitative analysis of gap area of HaCaT cells cultured on RHC, EGF, or RHC/EGF. (D) Optical micrographs of crystal violet stained NIH/3T3 cells adhering to monolayers presenting. (E) Quantitative detection of the number of NIH/3T3 cells adhering. (F) Cytoskeleton staining. (G) Quantitative calculation of cell spread area. n = 3, means ± SD, *P<0.05, **P<0.01 vs control group, ns means no significant difference vs. control, P >0.05.

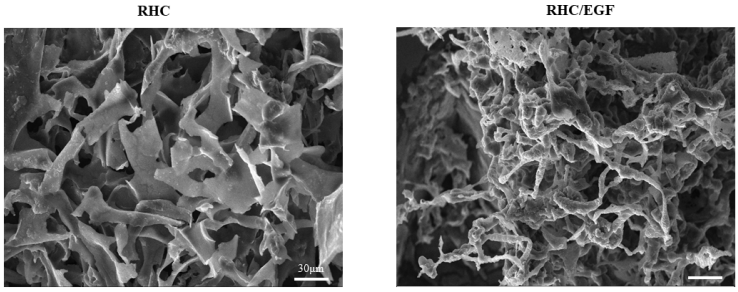

Fig. 3. Characteristics of RHC and RHC/EGF. (A) Scanning electron micrographs of RHC and RHC/EGF freeze-dried dressing

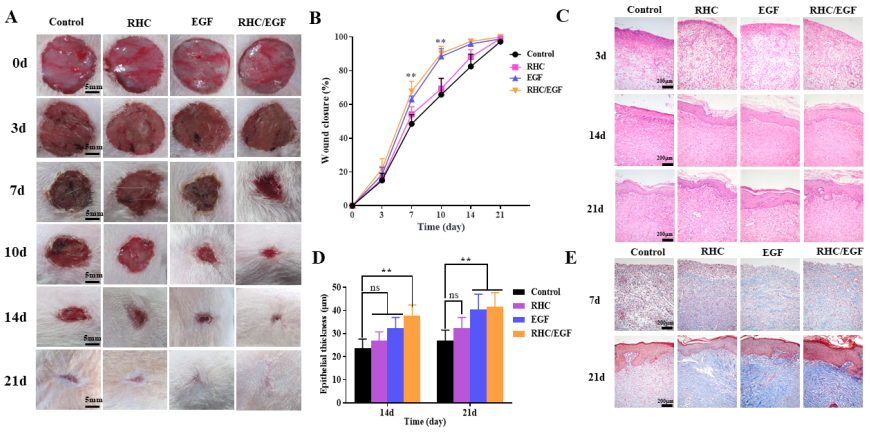

Fig. 4. Experimental study of rat wound-healing model after treatment with physiological saline, RHC, EGF, or RHC/EGF. (A) Wounds were photographed at 0, 3, 5, 7, 10, 14, and 21 d. (B) H&E staining of rat wound-healing model after treatment for 3, 14, and 21 d. (C) Quantitative analysis of epithelial thickness at 14 and 21 d using ImageJ software. (D) Quantitative analysis of wound closure rate. (E) Masson's trichrome staining of rat wound-healing model after treatment for 7 and 21 d. n = 6, means ± SD, *$P<0.05$, **$P<0.01$ *vs* control group, ns means no significant difference *vs.* control, $P>0.05$.

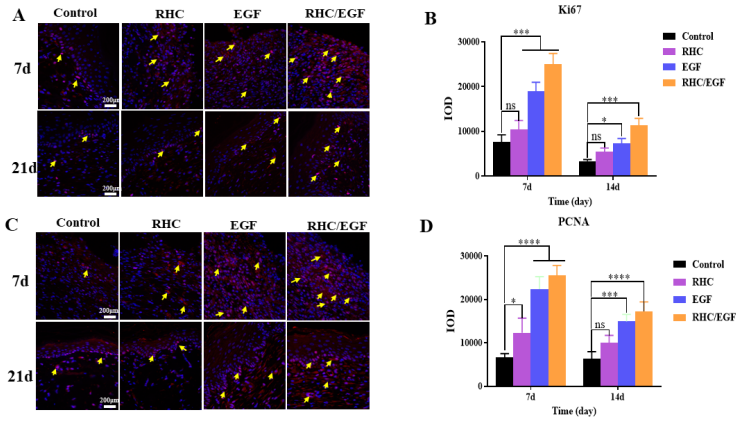

Fig. 5. Immunofluorescence examination of Ki67 and PCNA expression. (A) Immunofluorescence examination of Ki67-positive cells after treatment for 7 and 21 d. Arrows indicate Ki67 expression. (B) Quantitative analysis of Ki67-expressing cells at 7 and 14 d measured using ImageJ software. (C) Immunofluorescence examination of PCNA-positive cells after treatment for 7 and 21 d. Arrows indicate PCNA expression. (B) Quantitative analysis of PCNA-expressing cells at 7 and 14 d measured using ImageJ software. n = 3, means ± SD, *$P<0.05$, **$P<0.01$, ***$P<0.001$ vs control group, ns means no significant difference *vs.* control, $P>0.05$.

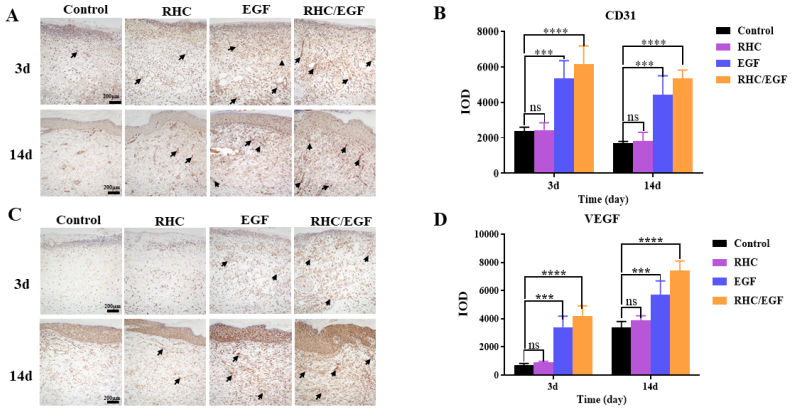

Fig. 6. Immunohistochemical examination of CD31 and VEGF expression. (A) Immunohistochemical labeling of CD31-positive cells after treatment for 3 and 14 d. Arrows indicate CD31 expression. (B) Quantitative analysis of CD31-expressing cells at 3 and 14 d measured using ImageJ software. (C) Immunohistochemical labeling of VEGF-positive cells after treatment for 3 and 14 d. Arrows indicate VEGF expression. (D) Quantitative analysis of VEGF-expressing cells measured at 3 and 14 d using ImageJ software. n = 3, means ± SD, *$P<0.05$, **$P<0.01$, ***$P<0.001$, ****$P<0.0001$ vs control group, ns means no significant difference *vs.* control, $P>0.05$.